Progress in Organic Coatings 97 (2016) 44–52

Contents lists available at ScienceDirect

Progress in Organic Coatings

journal homepage: www.elsevier.com/locate/porgcoat

Superhydrophobic, superoleophobic coatings for the protection of silk textiles

Dimitra Aslanidou [a], Ioannis Karapanagiotis [b,*], Costas Panayiotou [a,**]

[a] Department of Chemical Engineering, Aristotle University of Thessaloniki, 54124 Thessaloniki, Greece
[b] University Ecclesiastical Academy of Thessaloniki, Department of Management and Conservation of Ecclesiastical Cultural Heritage Objects, Thessaloniki 54250, Greece

ARTICLE INFO

Article history:
Received 17 October 2015
Received in revised form 25 February 2016
Accepted 9 March 2016
Available online 2 April 2016

Keywords:
Superhydrophobic
Superoleophobic
Supercritical CO_2
Silk
Textile
Cultural heritage

ABSTRACT

The fabrication of protective coatings on silk with special properties is presented. A water soluble siloxane emulsion enriched with silica nanoparticles (7 nm) is sprayed on silk, without the use of any organic solvent. By adjusting the nanoparticle concentration, treated silk obtains (i) superhydrophobic and superoleophobic properties, as evidenced by the high static contact angles of water and oil droplets (>150°) and (ii) water and oil repellent properties, as supported by the corresponding low tilt contact angles (<7°). SEM images show that nanoparticles lead to the formation of microscale clusters with nanostructures, which in turn induce a surface roughness at the micrometer and nanometer scale. The produced coatings have practically no effect on the aesthetic appearance of silk dyed with natural dyes such as indigo, weld, turmeric, and cochineal. Finally, it is shown that the applied coatings can be totally removed from the silk substrate using compressed carbon dioxide, either in supercritical or liquid state, mixed with a small amount of methanol. Consequently, the suggested method is reversible and therefore it has the potential to be used for the protection of modern as well as historic textiles.

1. Introduction

In the last two decades bioinspired surfaces of special wetting properties have attracted considerable attention e.g. [1,2]. Superhydrophobicity, accompanied by water repellency, is usually achieved by developing the special hierarchical micrometer and nanometer sized structure of the lotus leaf [3] on the surface of interest and applying low surface energy agents [4]. On the basis of these principles, and in relation to the final product application, several methods have been developed to fabricate superhydrophobic surfaces including, for instance, lithographic patterning [5,6], sol gel [7,8], layer by layer deposition [9], chemical vapor deposition [10], plasma etching [11] and nanoparticle deposition [12–16]. Moreover, green methods were developed using supercritical carbon dioxide for the fabrication of fluoropolymer nanoparticles [17] which were then used to produce superhydrophobic coatings [18,19].

Superomniphobic surfaces repel not only water, but virtually any liquid thrown on them. For practical applications, however, attention is mainly focused on oil and water repellency. The development of strategies to produce superomniphobic surfaces can be considered as the natural sequence of more than twenty years of research on superhydrophobic surfaces. Likewise with syperhydrophobicity, superomniphobicity is achieved by affecting appropriately both the surface geometry and surface chemical composition [20]. Consequently, the same techniques described above to achieve superhydrophobicity are roughly used to produce superoleophobic and superomniphobic materials and are, for instance, plasma treatment, self assembly, electrochemical deposition, magnetron sputtering deposition, chemical vapor deposition and polymer-nanoparticle coatings [21–35].

The textile industry has a special interest on superhydrophobic and superoleophobic materials as they can have an enormous impact on clothing and other textile products. Leng at al. [36] deposited charged micro- and nano-particles on cotton thus inducing a hierarchical structure. After the application of a perfluorodecyltrichlorosilane, the treated cotton obtained superhydrophobic properties [36]. Liu et al. produced superhydrophobic cotton using silica (SiO_2) nanoparticles and octadecyltrichlorosilane, as a low surface energy agent [37]. Hoefnagels et al. used also nanoparticles on cotton fibers to generate a dual-size sur-

* Corresponding author.
** Corresponding author.
E-mail addresses: y.karapanagiotis@aeath.gr (I. Karapanagiotis), cpanayio@auth.gr (C. Panayiotou).

http://dx.doi.org/10.1016/j.porgcoat.2016.03.013
0300-9440/

face roughness, while superhydrophobization was achieved using PDMS [38]. Artus et al. fabricated a superoleophobic polyester fabric coated with silicone nanofilaments and subsequent plasma fluorination [39]. Other researchers achieved the fabrication of superhydrophobic/superoleophobic textiles by layer by layer assembly [40], plasma treatment [39], sol-gel [41,42], chemical vapor phase deposition [43] and other methods [44–46].

In this work we present a simple, cost effective and green chemical method for the production of a coating on silk which shows both superhydrophobicity and superoleophocity accompanied by water and oil repellency. A water based emulsion of silane, siloxane and organic polymer is used and sprayed on silk. The resulting siloxane coating shows weak performance corresponding to relatively low/high static/tilt contact angles of water and oil droplets. However, the properties of the coating material are tuned by adding SiO_2 nanoparticles in the emulsion which enhance drastically both the hydrophobic and oleophobic character of the produced coating, increasing (>150°) and decreasing (<7°) the static and tilt contact angles, respectively, of both water and oil drops on treated silk. Dodecane droplets on treated silk are also studied to strengthen the reported observations. Furthermore, it is shown that the applied coatings can have negligible effects on the aesthetic appearance of dyed silk. The suggested method is designed to have the potential to be used for the protection of historic silk textiles of the cultural heritage. In 1963 Bradni published "La theoria del restauro" [47], where the basic principles of conservation science were introduced including reversibility which implies that any intervention on an object of the cultural heritage should be removable. We demonstrate that compressed carbon dioxide (CO_2), either in the supercritical or liquid state, mixed with a small amount of methanol (MeOH) is an effective solvent mixture which can remove the protective coatings from the silk substrate.

According to the above, the coating produced herein, (i) induces superhydrophobicity/superoleophocity accompanied by water/oil repellency on silk, (ii) is applied without using organic solvents, (iii) has practically no effect on the aesthetic appearance of dyed silk and (iv) can be removed by compressed CO_2. To the best of our knowledge, this is the first report where all these properties are combined in one product, designed for textile protection and conservation.

2. Materials and methods

Silres BS29A, a water soluble emulsion of silane, siloxane and organic polymer, was diluted in distilled water to prepare a stock solution of 7% wt. Silica (SiO_2) nanoparticles of 7 nm in mean diameter (Aldrich) were dispersed in the stock solution in various concentrations, that are 0.5%, 1%, 2%, 3%, 4% and 5% w/w. Dispersions were stirred vigorously for 30 min and sprayed onto clean 4 cm × 5 cm silk specimens, purchased from the local market. For comparison, pure Silres BS29A solution (without nanoparticles) was also sprayed on silk as well as clean glass slides. An airbrush system (Paasche Airbrush) with a nozzle of 660 μm diameter was used for the deposition of the dispersions and the solution. Each coating was produced by depositing 1 ml of the dispersion/solution while the airbrush was held at a distance of 20 cm from the silk surface (Fig. 1). Treated silk specimens were annealed at 40 °C overnight to remove residual solvent (water) and kept at room temperature for 2–3 days. It is noted that dispersions with nanoparticle concentration >5% w/w were too viscous and could not be deposited using the aforementioned Paasche airbrush system.

Static and tilt contact angles were measured on the surfaces of the treated silk specimens using an optical tensiometer apparatus (Attension Theta) and droplets of distilled water, olive oil (purchased from local market) and dodecane (Merck). Furthermore, contact angles of droplets, prepared using distilled water and hydrochloric acid (HCl) or sodium hydroxide (NaOH), corresponding to a pH range from 0.38 to 13.79, were measured. The reported contact angles are averages of five measurements. Variations are provided as error bars. The volume of the droplets was 8 μl.

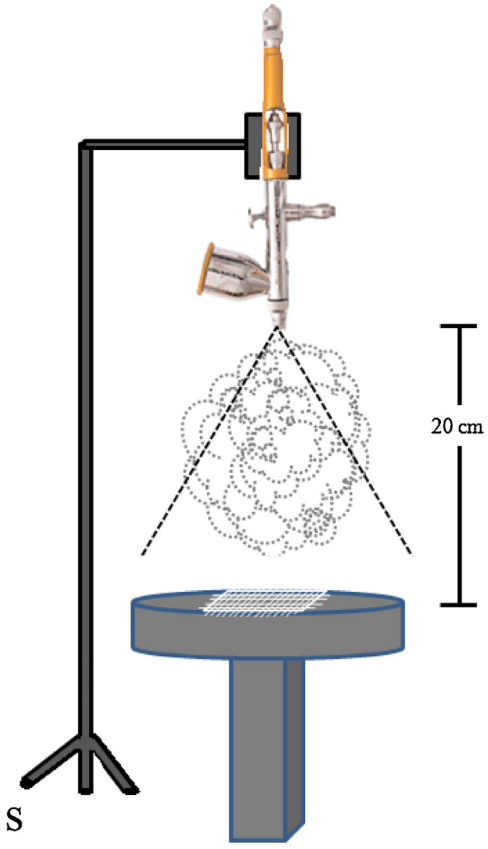

Fig. 1. Scheme of the experimental set up.

Scanning electron microscopy (SEM; JEOL, JSM-6510) was employed to study the surface structures of the treated silk specimens, which were coated with a thin layer of carbon. Colourimetric measurements were carried out using a Miniscan XE Plus spectrophotometer from Hunter Associates Laboratory Inc. and the results were evaluated using the L* a* b* coordinates of the CIE 1976 scale. The reported results are averages of three measurements. Colourimetric measurements were carried out on silk samples dyed with natural dyes such as indigo, weld, turmeric, and cochineal, as described in the Supplementary file.

Coated silk specimens were treated with carbon dioxide (CO_2), in supercritical (200 bar and 40 °C) and liquid (200 bar and 25 °C) state, to evaluate its efficacy to remove the applied coatings from silk. Small amounts of methanol (MeOH) were added in the solvent mixture. The experimental high pressure apparatus is described in detail elsewhere [48–50]. Briefly, a syringe pump (ISCO 100DX) compresses CO_2 and transfers it inside a high-pressure cell (volume of 40 ml). A perforated metallic support, which holds the sample, is positioned inside the cell. Once the sample is set inside the cell, the cell is sealed, carbon dioxide is admitted inside the cell and the pressure rises, up to the desired point. Once the cleaning is completed, decompression takes place and the sample is removed from the cell. The cleaning results are evaluated by weight loss measurements using a Sartorius balance (model B120) with an accuracy of 0.0001 g. After decompression, some treated silk specimens were blown with compressed (1.5 bar) air for 2 min to achieve total removal of the coatings from the silk substrate.

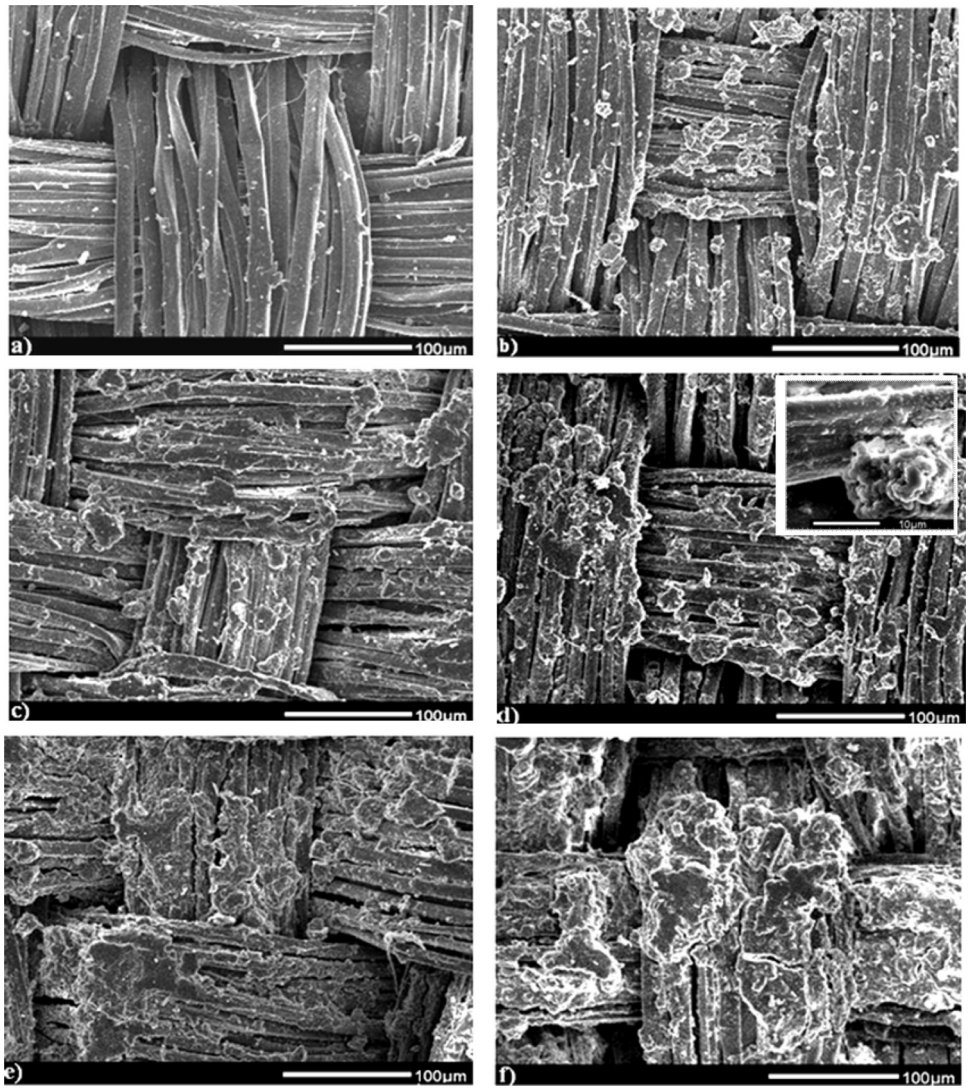

Fig. 2. SEM images of siloxane (Silres BS29A) coatings enriched with SiO_2 nanoparticles on silk. Coatings were prepared using the following SiO_2 nanoparticle concentrations: (b) 1% w/w, (c) 2% w/w, (d) 3% w/w, (e) 4% w/w and (f) 5% w/w. In (a) the surface of the film produced using only pure siloxane (without SiO_2 nanoparticles) is shown.

3. Results and discussion

3.1. Surface structures of the coatings

The SEM images of Fig. 2 reveal the effect of the SiO_2 nanoparticle concentration on the surface structures of the coatings, deposited on silk. When the silk substrate is covered by pure siloxane (Fig. 2a) there is no significant surface structure originated by the deposited coating. The use of nanoparticles results in the formation of microscale clusters with nanostructures, which in turn induce a surface roughness at the micrometer and nanometer scale. Initially, the clusters are separated by large areas with no special structure (Fig. 2b and c). Larger, coalesced and higher clusters are formed gradually as the particle concentration increases (Fig. 2d–f). The scenario revealed in Fig. 2 is in perfect agreement with previously published studies which described the effect of nanoparticles on the surface of polymer-nanoparticle composite films [51–54].

3.2. Contact angles

Fig. 3 shows measurements of static (θ_s) and tilt (θ_t) contact angles of water, oil and dodecane droplets on treated silk as a function of the SiO_2 nanoparticle concentration. Attention is first focused on the results reported for water (Fig. 3a) and oil (Fig. 3b) droplets, which are important for practical applications. Silk samples treated with pure siloxane correspond to θ_s of 147.8° (Fig. 3a) and 140° (Fig. 3b) for droplets of water and oil, respectively. These values are high compared to the θ_s measured when pure siloxane was deposited on smooth glass: $\theta_s = 80°$ for water and $\theta_s = 43°$ for oil droplets on treated glass. It is therefore concluded that the intrinsic roughness of the knitted silk fibers plays a key role [55] in enhancing both the hydrophobic and oleophobic character of the deposited coating.

Both Fig. 3a and b show that θ_s increases with nanoparticle concentration. Superhydrophobicity (θ_s of water droplets > 150°) is achieved at the SiO_2 concentration of 0.5% w/w, according to the results of Fig. 3a. However, θ_s keeps increasing with nanoparticle concentration until this becomes 1% w/w. Further increase in SiO_2 concentration (>1% w/w) does not have any significant effect on θ_s which is (i) stable, corresponding to the plateau of the curve in Fig. 3a and (ii) extremely large (around 161°). The behavior of the θ_s curve in Fig. 3a is in agreement with previously published studies which described the effect of nanoparticle additives on the wettability of polymer surfaces [51–54].

The variation of θ_s of oil droplets is more complicated, as evidenced by the results of Fig. 3b. Treated silk reaches

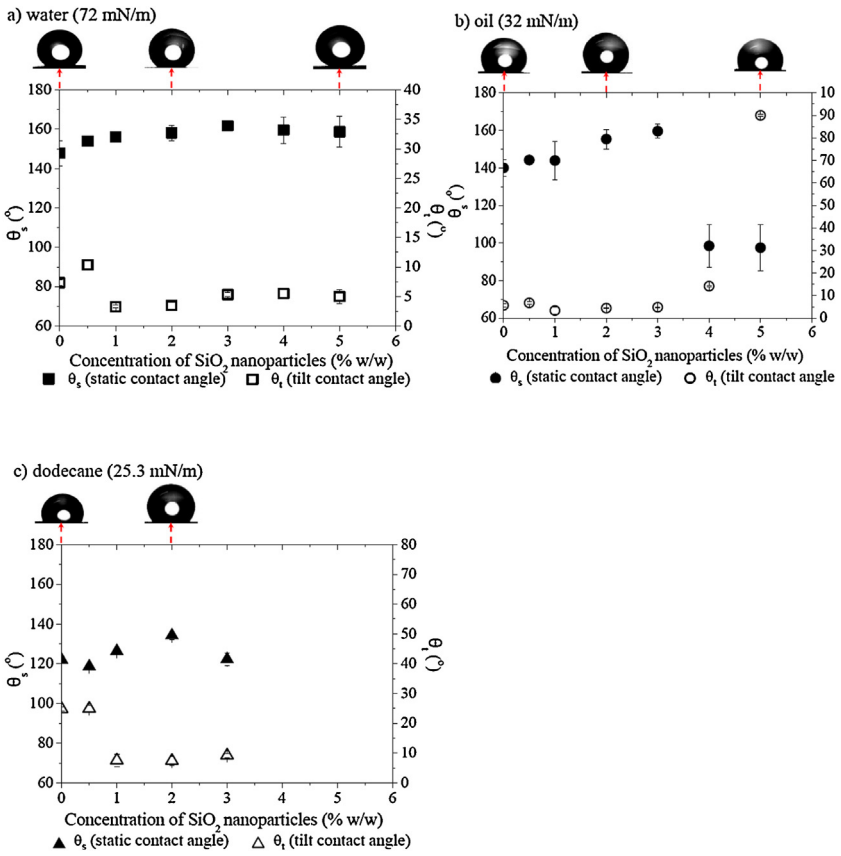

Fig. 3. Static (θ_s) and tilt (θ_t) contact angles of (a) water, (b) oil and (c) dodecane droplets vs the concentration of SiO_2 nanoparticles. Photographs of selected water, oil and dodecane droplets are included. Surface tensions of the tested liquids are provided in parentheses.

superoleophobicity (θ_s of oil droplets > 150°) at the nanoparticle concentration of 2% w/w. The angle is high and roughly stable for a short nanoparticle concentration range (2–3% w/w). Further increase in SiO_2 concentration (>3% w/w) results in a rapid decrease of θ_s according to the results of Fig. 3b, which shows that θ_s becomes around 97 ° for 4 and 5%w/w nanoparticle concentration.

Because the behavior reported in Fig. 3b for oil droplets is rather surprising, experiments were repeated using dodecane which has a surface tension (=25.3 mN/m) comparable to that of oil (=32 mN/m). The results for dodecane droplets are presented in Fig. 3c: initially θ_s increases with nanoparticle concentration, it reaches a maximum value (=134.2° at 2% w/w) and then decreases. Consequently, the decrease of θ_s at elevated nanoparticle concentration is recorded for both oil (Fig. 3b) and dodecane (Fig. 3c) droplets. It is noted, that dodecane droplets were absorbed by coatings prepared with nanoparticle concentration of 4 and 5% w/w and therefore θ_s measurements on these surfaces are not reported in Fig. 3c.

Interestingly, the maxima θ_s measured for the three tested liquids in Fig. 3 follow the sequence water (=161°) > oil (=159°) > dodecane (=134°) implying that the largest/smallest θ_s was obtained for the liquid droplets of the highest/lowest surface tension, that is water (=72 mN/m)/dodecane (=25.3 mN/m). The same sequence applies on the duration of the plateaus of the curves of Fig. 3: the long plateau in Fig. 3a (water droplets) holds for nanoparticle concentration >1% w/w and the hardly defined plateau in Fig. 3b (oil droplets) is narrow as it is extended only within the nanoparticle concentration range of 2–3% w/w. In Fig. 3c (dodecane droplets) there is practically no plateau.

Measurements of θ_t of water, oil and dodecane droplets are included in Fig. 3. The variation of θ_t for water droplets (Fig. 3a) is in agreement with previously published reports which described the effect of nanoparticles on the surface of polymer-nanoparticle composite films [8,12–16,52]. According to the results of Fig. 3a, as the nanoparticle concentration increases we first record an increase in θ_t, which reaches a maximum value (10.4° for 0.5% w/w) and then decreases. At the particle concentration of 1% w/w, θ_t is minimized (<7°) and becomes roughly constant.

The θ_t of oil droplets (Fig. 3b) show initially a similar variation with a slight increase at 0.5% w/w followed by a decrease of θ_t (<7°) reported for surfaces corresponding to 1, 2 and 3% w/w. However, at 4% w/w an increase of θ_t (=14.2°) for the oil droplets is observed which is pronounced at 5% w/w where oil droplets are pinned and can roll off the surface only when this is turned by almost 90°. This increase of θ_t is accompanied by a decrease of θ_s (Fig. 3b).

For dodecane droplets (Fig. 3c) θ_t decreases from around 25° (no particles and 0.5% w/w particle concentration) to 7° at 1% w/w particle concentration. A very slight increase is recorded at 3% w/w (θ_t = 9°) which is the last measurement that could be reported, as dodecane was absorbed by coatings, which were prepared using 4 and 5% w/w nanoparticles.

As mentioned above, the results in Fig. 3a which describe the interaction of water droplets with the substrate are in agreement with previously published reports [8,12–16,51] and can be explained if we consider the effect of the nanoparticles on the morphology of the deposited coating, revealed in the SEM image of Fig. 2. Microscale clusters are separated by large areas in Fig. 2b and 2c corresponding to coatings prepared using low particle concentration. The water droplet fills these large areas existing among the clusters. In this case, clusters act as pinning sites resulting in an increase of θ_t. However, it is quite possible that water does not penetrate the nanocrevices that exist on the surface of the protruding clusters because of the Laplace pressure. At elevated particle

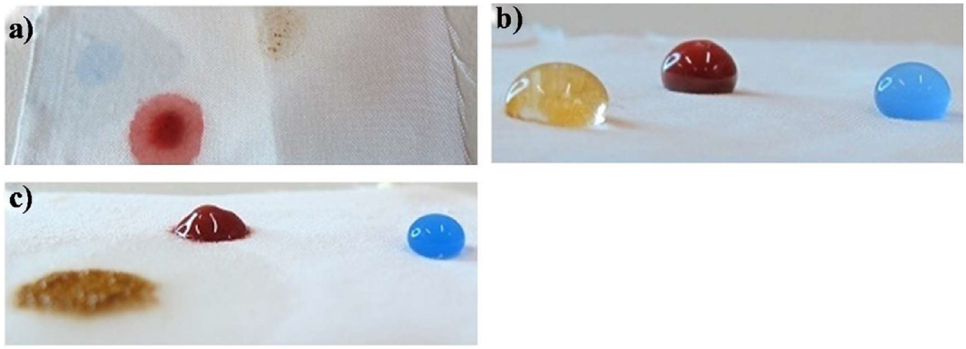

Fig. 4. Photographs of silk (a) untreated, (b) covered by siloxane enriched with 2% w/w SiO_2 and (c) covered by siloxane enriched with 5% w/w SiO_2. Droplets of water (coloured blue), olive oil (coloured red) and dodecane (coloured yellow) were placed on the three surfaces. (For interpretation of the references to colour in this figure legend, the reader is referred to the web version of this article.)

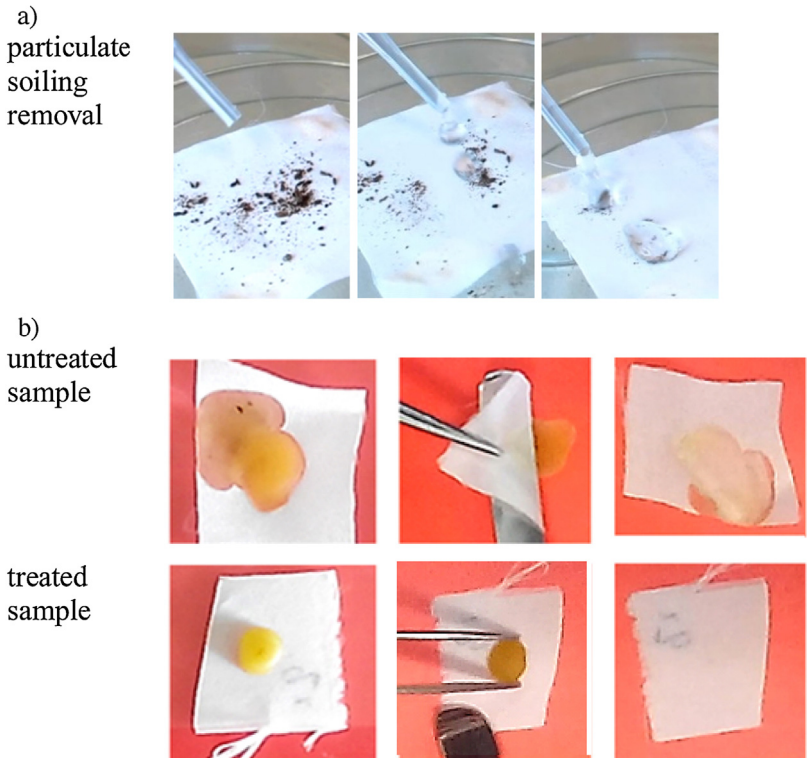

Fig. 5. Self/easy cleaning properties of silk covered by siloxane enriched with 2% w/w SiO_2 nanoparticles. The easy removal of soil by water droplets is demonstrated in (a). The mechanical removal of wax is shown in (b) for untreated and treated (siloxane + 2% w/w SiO_2) silk.

concentrations (Fig. 2d–f) the clusters become dense forming thus a continuous rough surface resulting in high and low θ_s and θ_t for water droplets, respectively. Superhydrophobicity and water repellency are sustained by any surface corresponding to particle concentration >1% w/w.

However, superoleophobicity and oil repellency collapse at the concentration of 4% w/w, according to the results of Fig. 3b, implying that the low surface tension oil droplet sinks into the rough surface thus corresponding to a transition from the non-sticking, repellent state to the droplet-pinned state. A breakdown of superoleophobicity on structured surfaces was described in earlier studies [56–59]. The same behavior is reported in Fig. 3c for dodecane droplets.

Figs. 4 and 5 demonstrate the above described wetting properties. In particular, Fig. 4 shows photographs of static droplets on untreated (Fig. 4a) and treated (Fig. 4b and c) silk and Fig. 5 demonstrates the self-/easy-cleaning properties of silk, treated with appropriate coatings. Any liquid is absorbed by the untreated silk as shown in Fig. 4a. Superhydrophobicity and superoleophobicity are achieved when silk is covered by a siloxane + 2% w/w SiO_2 coating (Fig. 4b). The dodecane droplet corresponds also to a very high contact angle in Fig. 4b. Superoleophobicity collapses in Fig. 4c, which shows droplets on silk coated by a siloxane + 5% w/w SiO_2, but superhydrophobicity is maintained. Dodecane is absorbed by the treated silk in Fig. 4c.

In Fig. 5a the easy removal of soil by water droplets is demonstrated for silk covered by a siloxane + 2% w/w SiO_2 coating. In Fig. 5b, the removal of waxy soil is investigated. A small amount of wax was poured and dried on untreated silk and silk treated with siloxane + 2% w/w SiO_2. As shown in Fig. 5b, the wax is easily removed mechanically from the treated sample without leaving

Table 1
Total colour difference (ΔE^*) of undyed and dyed silk covered by various siloxane + SiO_2 coatings.

Concentration of SiO_2 (% w/w)	ΔE^*				
	undyed silk	silk dyed with indigo	silk dyed with weld	silk dyed with turmeric	silk dyed with cochineal
0 (pure siloxane)	2.44 ± 0.83	3.27 ± 0.52	4.27 ± 0.36	4.41 ± 0.98	3.03 ± 0.36
1	2.05 ± 0.9	1.02 ± 0.67	1.58 ± 0.4	2.10 ± 0.68	1.44 ± 0.63
2	5.71 ± 2.03	3.03 ± 0.98	1.59 ± 0.63	12.25 ± 2.5	8.05 ± 1.1
3	9.81 ± 2.26	17.77 ± 0.83	8.81 ± 1.07	50.02 ± 2.69	28.24 ± 0.83

any residual wax on the textile surface. However, a stain is left on the surface of the untreated silk upon wax removal.

Finally, the durability of the hierarchically rough coatings (siloxane + 2% w/w SiO_2) over a wide range of pH is demonstrated in Fig. 6. For comparison, results collected on silk treated with pure siloxane are included in Fig. 6. Both surfaces maintain their wetting properties over the pH range except for extreme basic conditions (pH = 13.79) where a slight decrease in θ_s is observed. Superhydrophobicity is maintained in the composite (siloxane + 2% w/w SiO_2) coating because the siloxane material exhibits a good stability over pH.

3.3. Colourimetry

Coatings applied on the surface of dyed textiles for protection must not affect the aesthetic appearance of the treated textile substrate. To evaluate the effect of the siloxane-nanoparticle coatings on the appearance of silk, colourimetric measurements were carried out using the L*a*b* coordinates of the CIE 1976 scale. The global colour differences (ΔE^*) of the silk surface, raised by the application of a protective coating, was calculated according to Eq. (1):

$$\Delta E^* = \sqrt{\Delta L^{*2} + \Delta a^{*2} + \Delta b^{*2}} \quad (1)$$

where, L*, a* and b* are the brightness (0 for black–100 for white), the red–green component (positive for red and negative for green) and the yellow–blue component (positive for yellow and negative for blue), respectively.

Colourimetric measurements were carried out on undyed silk and silk dyed with natural dyes, which have been commonly used and identified in textiles of the cultural heritage, that is indigo (blue dye), weld, turmeric (yellow dyes) and cochineal (red dye) [60]. Dyeing recipes applied for the preparation of the samples are described in the Supplementary file. The ΔE^* measurements for the undyed and dyed silk samples treated with pure siloxane and siloxane with nanopaticles at different concentrations are summarised in Table 1. Fig. 7 is provided as an example showing in detail the measurements corresponding to silk dyed with indigo.

Fig. 7 shows that the application of pure siloxane on silk dyed with indigo caused a colour change (ΔE^* = 3.27 according to Table 1) that is primarily attributed to the change of the brightness component (L*). The application of pure siloxane had a similar effect on the appearances of undyed silk and silk dyed with weld, turmeric and cochineal, according to the results of Table 1.

The addition of SiO_2 nanoparticles in the protective coatings at the low concentration of 1% w/w had a positive effect, as the ΔE^* values reduced from that of the silk specimens treated with pure siloxane (Table 1). The colour changes imposed by the application of siloxane + 1%w/w SiO_2 correspond to values lower the JND (Just Noticeable Difference) limit of 2.3 [48], thus implying that the use of these coatings do not affect practically the aesthetic appearances of the treated silk specimens. However, the use of more SiO_2 nanoparticles (2 and 3% w/w) in the protective coating results in larger ΔE^* values, according to the results of Table 1.

Table 2
Colour coordinates of SiO_2 nanoparticles and silk samples (undyed and dyed).

Material	L*	a*	b*
SiO_2	88.00	−2.50	−7.00
Undyed silk	76.02	−0.04	1.02
Silk dyed with indigo	33.75	−4.14	−16.08
Silk dyed with weld	74.56	−1.56	7.47
Silk dyed with turmeric	74.03	−3.12	63.40
Silk dyed with cochineal	23.26	28.04	3.81

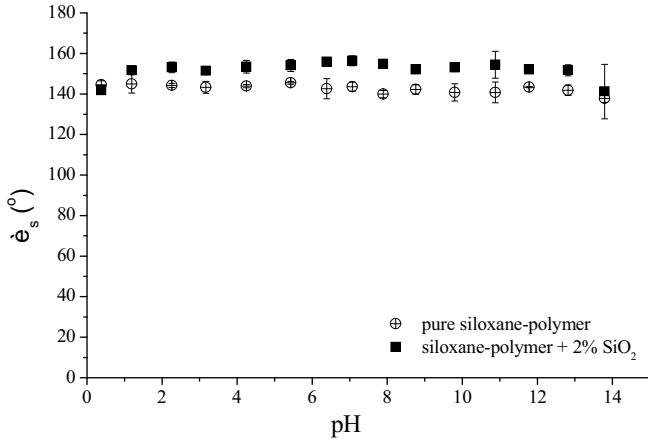

Fig. 6. Contact angle (θ_s) versus the pH of droplets which were placed on silk covered by pure siloxane-polymer (without particles) and siloxane-polymer enriched with 2% w/w SiO_2 nanoparticles.

The effect of the SiO_2 nanoparticles is more pronounced in silk dyed with turmeric, indigo and cochineal because the colour coordinates of these dyes are substantially different compared to the corresponding values measured for SiO_2, according to Table 2. However, the colour components for SiO_2 are relatively close to the corresponding values reported for undyed silk and silk dyed with weld (Table 2). Consequently, the effect of the SiO_2 nanoparticles on the colour appearance of these two samples is smaller.

In summary, the results of Table 1 suggest that the use of siloxane +1%w/w SiO_2 for the protection of undyed and dyed silk is appropriate and does not cause any colour change noticeable by human eye. At the 2% w/w nanoparticle concentration, the coatings correspond to higher ΔE^* (Table 2) but also to somewhat better water and oil repellence, evidenced by the results of Fig. 3a and b.

3.4. Removal of the superhydrophobic/superoleophobic coatings using CO_2

We have recently developed a green method for textile (silk and cotton) cleaning, using supercritical CO_2 at 200 bar and 40 °C [48]. Dirt removal from silk was on the order of 53–97% and this was achieved without affecting natural dyes, such as indigo, weld, turmeric, and cochineal, which were applied on the textile specimens [48]. The previously devised method is

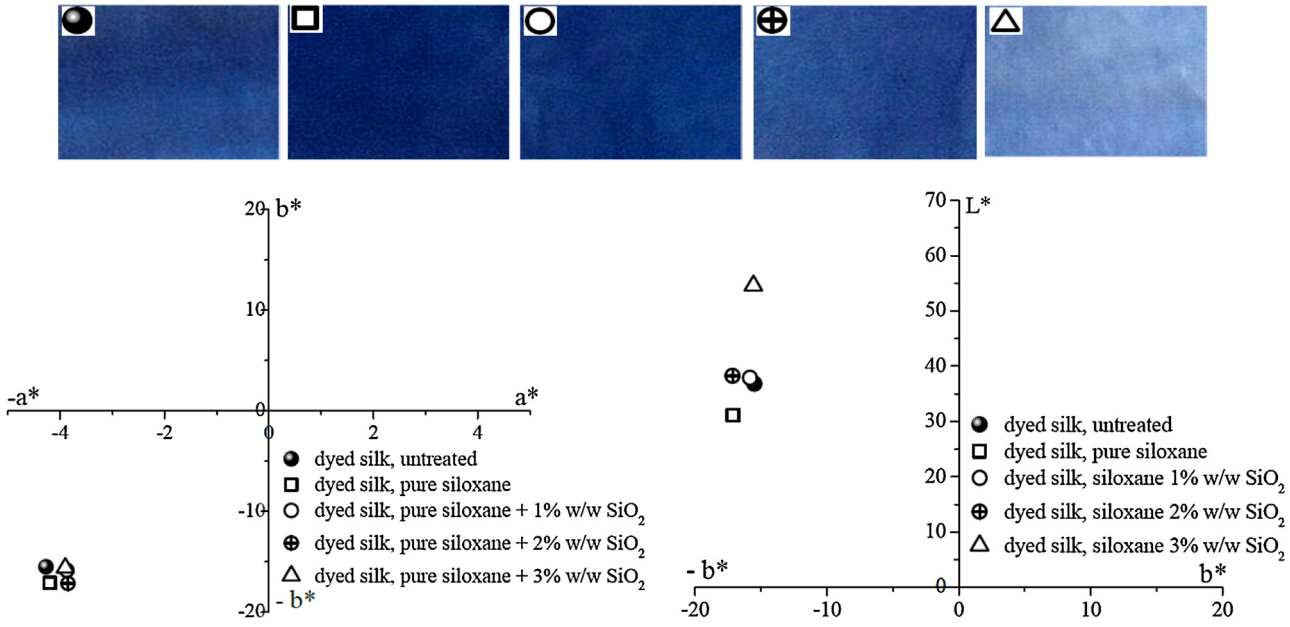

Fig. 7. L*, a*, b* coordinates measured for silk dyed with indigo: (●) untreated silk and silk covered by (□) pure siloxane, (○) siloxane + 1% w/w SiO_2 nanoparticles, (⊕) siloxane + 2% w/w SiO_2 nanoparticles and (△) siloxane + 3% w/w SiO_2 nanoparticles. Photographs of the samples are provided above.

Table 3
Pressure (P) and temperature (T) of the CO_2 and MeOH solvent mixtures which were used to remove siloxane + 2% w/w SiO_2 coatings from silk. The reported % removals were measured by means of weight losses.

P (bar)	T (°C)	% (v/v) MeOH	xMeOH	xCO_2	% removal
200	40	0	0	1	37.4 ± 7.9
200	40	5	0.061	0.939	72.4 ± 8.3
200	40	10	0.114	0.885	63.7 ± 8.1
200	25	5	0.057	0.943	73.2 ± 9.3
200	25	10	0.108	0.892	48.6 ± 10.1
200	25	20	0.195	0.805	36.1 ± 4.2

applied herein to evaluate its efficacy to remove the superhydrophobic/superoleophobic siloxane + SiO_2 coatings from silk. As described in Table 3, a 37.4% removal of the composite coating was achieved when pure supercritical CO_2 (at 200 bar and 40 °C) was used. To improve this rather poor yield, the original method [48] was slightly modified by adding small amounts of MeOH (5 and 10% v/v) as co-solvent. This additional step resulted in better % removals (72.4 and 63.7, respectively) according to Table 3.

In a second step, the temperature of the CO_2 + MeOH solvent mixture was reduced from 40 to 25 °C. High treatment temperatures can have negative side effects on dyed silk fibers and therefore they should be avoided. Under the new conditions (200 bar and 25 °C) CO_2 is in the liquid state. According to the results of Table 3, temperature reduction did not have any effect on the cleaning efficacy of the CO_2 + MeOH (5%v/v) mixture. A 73.2% removal was obtained at 25 °C which is practically the same with the 72.4% yield reported at 40 °C. Interestingly, the cleaning efficacy of the solvent mixture was reduced when elevated percentages of MeOH (10 and 20% v/v) were used, thus suggesting that CO_2 plays a key role in the cleaning procedure. It should be expected that the low viscosity and high diffusivity of CO_2 allows a deep penetration of the solvent mixture into the structure of the coating which in turn is removed easier. The removal of the coating from silk is due to the effects of the solvent mixture (chemical removal) and the decompression step (mechanical removal).

Finally, a third step was added in the suggested method that resulted in the total removal of the siloxane + SiO_2 coating from silk: after the treatment with CO_2 + MeOH (5%v/v) at 200 bar and 25 °C and the subsequent decompression step, the specimen was blown with compressed (1.5 bar) dry air for 2 min. It is reported that 100% removal of the coating was achieved. It is stressed that compressed air did not have any effect without the application of the CO_2 + MeOH treatment which (i) removed most (73.2%) of the siloxane + SiO_2 and (ii) contributed to the detachment of the remaining coating from the silk substrate. The poorly adhered remaining coating was easily and totally removed from silk by compressed air. Consequently, the application of the superhydrophobic/superoleophobic siloxane-SiO_2 coatings on silk is an absolutely reversible treatment method which has the potential to be used in modern conservation science of historic textiles.

4. Conclusions

Superhyrophobicity, superoleophobicity, water and oil repellency were induced on silk by applying coatings composed of a water-borne siloxane enriched with SiO_2 nanoparticles. The film deposition on silk was carried out by a simple spraying technique. The effects of the nanoparticle concentration on the static and tilt contact angles of water and oil droplets were studied in detail. The aforementioned extreme wetting properties were obtained by adjusting the concentration of the nanoparticles which according to SEM images lead to the formation of microscale clusters with nanostructures. Treated silk obtained self-/easy-cleaning properties and maintained its wetting properties for a wide range of pH of water droplets.

Moreover, it was shown that the siloxane + SiO_2 composite coatings have practically no effect on the aesthetic appearance of silk dyed with natural dyes such as indigo, weld, turmeric, and cochineal which have been commonly used in historic textiles.

The suggested method is extremely easy, friendly to the user and the environment (no organic solvent is used), can be applied to treat large textile surfaces and it is of low cost considering that it does not include the use of sophisticated instrumentation.

Finally, it was shown that the applied coatings can be totally removed from the silk substrate using compressed carbon dioxide mixed with a small amount of methanol. Consequently, the method

is reversible and therefore it has the potential to be used in modern conservation science of historic textiles.

Appendix A. Supplementary data

Supplementary data associated with this article can be found, in the online version, at http://dx.doi.org/10.1016/j.porgcoat.2016.03.013.

References

[1] S. Nishimoto, B. Bhushan, Bioinspired self-cleaning surfaces with superhydrophobicity, superoleophobicity, and superhydrophilicity, RSC Adv. 3 (2013) 671–690.
[2] S. Pechook, N. Kornblum, B. Pokroy, Superoleophobic materials bio-inspired superoleophobic fluorinated wax crystalline surfaces, Adv. Funct. Mater. 23 (2013) 4572–4576.
[3] W. Barthlott, C. Neinhuis, Purity of the sacred lotus, or escape from contamination in biological surfaces, Planta 202 (1997) 1–8.
[4] E. Celia, T. Darmanin, E. Taffin de Givenchy, S. Amigoni, F. Guittard, Recent advances in designing superhydrophobic surfaces, J. Colloid Interf. Sci. 402 (2013) 1–18.
[5] B. Bhushan, K. Koch, Y.C. Jung, Fabrication and characterization of the hierarchical structure for superhydrophobicity and self-cleaning, Ultramicroscopy 109 (2009) 1029–1034.
[6] I. Bernagozzi, S. Torrengo, L. Minati, M. Ferrari, A. Chiappini, C. Armellini, L. Toniutti, L. Lunelli, G. Speranza, Synthesis and characterization of PMMA based superhydrophobic surfaces, Colloid Polym. Sci. 290 (2012) 315–322.
[7] R.V. Lakshmi, T. Bharathidasan, B.J. Basu, Superhydrophobic sol–gel nanocomposite coatings with enhanced hardness, Appl. Surf. Sci. 257 (2011) 10421–10426.
[8] I. Karapanagiotis, A. Pavlou, P.N. Manoudis, K.E. Aifantis, Water repellent ORMOSIL films for the protection of stone and other materials, Mater. Lett. 131 (2014) 276–279.
[9] T. Wang, T.T. Isimjan, J. Chen, S. Rohani, Transparent nanostructured coatings with UV-shielding and superhydrophobicity properties, Nanotechnology 22 (2011), Article ID 265708.
[10] Y. Li, Z. Zhang, X. Zhu, X. Men, B. Ge, X. Zhou, Fabrication of a superhydrophobic coating with high adhesive effect to substrates and tunable wettability, Appl. Surf. Sci. 328 (2015) 475–481.
[11] H.C. Barshilia, N. Gupta, Superhydrophobic polytetrafluoroethylene surfaces with leaf-like micro-protrusions through Ar+ O 2 plasma etching process, Vacuum 99 (2014) 42–48.
[12] I. Karapanagiotis, D. Grosu, D. Aslanidou, K.E. Aifantis, Facile method to prepare superhydrophobic and water repellent cellulosic paper, J. Nanomater. (2015), Article ID 219013.
[13] P.N. Manoudis, I. Karapanagiotis, Modification of the wettability of polymer surfaces using nanoparticles, Prog. Org. Coat. 77 (2014) 331–338.
[14] A. Chatzigrigoriou, P.N. Manoudis, I. Karapanagiotis, Fabrication of water repellent coatings using waterborne resins for the protection of the cultural heritage, Macromol. Symp. 331–332 (2013) 158–165.
[15] I. Karapanagiotis, P.N. Manoudis, A. Savva, C. Panayiotou, Superhydrophobic polymer-particle composite films produced using various particle sizes, Surf. Interface Anal. 44 (2012) 870–875.
[16] P.N. Manoudis, I. Karapanagiotis, A. Tsakalof, I. Zuburtikudis, B. Kolinkeová, C. Panayiotou, Superhydrophobic films for the protection of outdoor cultural heritage assets, Appl. Phys. A Mater. 97 (2009) 351–360.
[17] S. Khapli, R. Jagannathan, Supercritical CO2 based processing of amorphous fluoropolymer Teflon-AF: surfactant-free dispersions and superhydrophobic films, J. Supercrit. Fluids 85 (2014) 49–56.
[18] L. Ovaskainena, I. Rodriguez-Meizoso, N.A. Birkin, St M. Howdle, U. Gedde, L. Wågberg, C. Turner, Towards superhydrophobic coatings made by non-fluorinated polymers sprayed from a supercritical solution, J. Supercrit. Fluids 77 (2013) 134–141.
[19] C. Quana, O. Werner, L. Wågberg, C. Turner, Generation of superhydrophobic paper surfaces by a rapidly expanding alkyl ketene dimer—supercritical carbon dioxide solution, J. Supercrit. Fluids 49 (2009) 117–124.
[20] K. Liu, Y. Tian, L. Jiang, Bio-inspired superoleophobic and smart materials: design, fabrication, and application, Prog. Mater. Sci. 58 (2013) 503–564.
[21] L. Cao, T.P. Price, M. Weiss, D. Gao, Super water- and oil-repellent surfaces on intrinsically hydrophilic and oleophilic porous silicon films, Langmuir 24 (2008) 1640–1643.
[22] A. Tuteja, W. Choi, J.M. Mabry, G.H. McKinley, R.E. Cohen, Robust omniphobic surfaces, Proc. Natl. Acad. Sci. U. S. A. 105 (2008) 18200–18205.
[23] W. Choi, A. Tuteja, S. Chhatre, J.M. Mabry, R.E. Cohen, G.H. McKinley, Fabrics with tunable oleophobicity, Adv. Mater. 21 (2009) 2190–2195.
[24] A.K. Kota, Y. Li, J.M. Mabry, A. Tuteja, Hierarchically structured superoleophobic surfaces with ultralow contact angle hysteresis, Adv. Mater. 24 (2012) 5838–5843.
[25] P. Kim, T.-S. Wong, J. Alvarenga, M.J. Kreder, W.E. Adorno-Martinez, J. Aizenberg, Liquid-infused nanostructured surfaces with extreme anti-ice and anti-frost performance, ACS Nano 6 (2012) 6569–6577.
[26] A. Lafuma, D. Quéré, Slippery pre-suffused surfaces, Europhys. Lett. 96 (2011), Article ID 56001.
[27] T.S. Wong, S.H. Kang, S.K.Y. Tang, E.J. Smythe, B.D. Hatton, A. Grinthal, J. Aizenberg, Bioinspired self-repairing slippery surfaces with pressure-stable omniphobicity, Nature 477 (2011) 443–447.
[28] D. Richard, D. Quéré, Bouncing water drops, Europhys. Lett. 50 (2000) 769–775.
[29] Y. Wu, B. Su, L. Jiang, A.J. Heeger, Liquid-liquid-solid-type superoleophobic surfaces to pattern polymeric semiconductors towards high-quality organic field-effect transistors, Adv. Mater. 25 (2013) 6526–6533.
[30] E. Bormashenko, R. Grynyov, G. Chaniel, H. Taitelbaum, Y. Bormashenko, Robust technique allowing manufacturing superoleophobic surfaces, Appl. Surf. Sci. 270 (2013) 98–103.
[31] S. Pechook, N. Kornblum, B. Pokroy, Bio-inspired superoleophobic fluorinated wax crystalline surfaces, Adv. Funct. Mater. 23 (2013) 4572–4576.
[32] T. Fujii, Y. Aoki, H. Habazaki, Fabrication of super-oil-repellent dual pillar surfaces with optimized pillar intervals, Langmuir 27 (2011) 11752–11756.
[33] T. Darmanin, F. Guittard, S. Amigoni, E.T. de Givenchy, X. Noblin, R. Kofman, F. Celestini, Superoleophobic behavior of fluorinated conductive polymer films combining electropolymerization and lithography, Soft Matter 7 (2011) 1053–1057.
[34] A. Steele, I. Bayer, E. Loth, Inherently superoleophobic nanocomposite coatings by spray atomization, Nano Lett. 9 (2009) 501–505.
[35] Y.C. Sheen, W.H. Chang, W.C. Chen, Y.H. Chang, Y.C. Huang, F.C. Chang, Non-fluorinated superamphiphobic surfaces through sol–gel processing of methyltriethoxysilane and tetraethoxysilane, Mater. Chem. Phys. 114 (2009) 63–68.
[36] B.X. Leng, Z.Z. Shao, G. de With, W.H. Ming, Superoleophobic cotton textiles, Langmuir 25 (2009) 2456–2460.
[37] F. Liu, M. Ma, D. Zang, Z. Gao, C. Wang, Fabrication of superhydrophobic/superoleophilic cotton for application in the field of water/oil separation, Carbohydr. Polym. 103 (2014) 480–487.
[38] H.F. Hoefnagels, D. Wu, G. de With, W. Ming, Biomimetic superhydrophobic and highly oleophobic cotton textiles, Langmuir 23 (2007) 13158–13163.
[39] G.R.J. Artus, J. Zimmermann, F.A. Reifler, S.A. Brewer, S. Seeger, A superoleophobic textile repellent towards impacting drops of alkanes, Appl. Surf. Sci. 258 (2012) 3835–3840.
[40] M. Zhang, S. Wang, C. Wang, J. Li, A facile method to fabricate superhydrophobic cotton fabrics, Appl. Surf. Sci. 261 (2012) 561–566.
[41] Y. Shi, Y. Wang, X. Feng, G. Yue, W. Yang, Fabrication of superhydrophobicity on cotton fabric by sol–gel, Appl. Surf. Sci. 258 (2012) 8134–8138.
[42] H. Wang, Y. Xue, T. Lin, One-step vapour-phase formation of patternable electrically conductive, superamphiphobic coatings on fibrous materials, Soft Matter 7 (2011) 8158–8161.
[43] X. Zhou, Z. Zhang, X. Xu, X. Men, X. Zhu, Fabrication of super-repellent cotton textiles with rapid reversible wettability switching of diverse liquid, Appl. Surf. Sci. 276 (2013) 571–577.
[44] R. Saraf, H.J. Lee, S. Michielsen, J. Owens, C. Willis, C. Stone, E. Wilusz, Comparison of three methods for generating superhydrophobic, superoleophobic nylon nonwoven surface, J. Mater. Sci. 46 (2011) 5751–5760.
[45] R.A. Hayn, J.R. Owens, S.A. Boyer, R.S. McDonald, H.J. Lee, Preparation of highly hydrophobic and oleophobic textile surfaces using microwave-promoted silane coupling, J. Mater. Sci. 46 (2011) 2503–2509.
[46] M.A. Shirgholami, M.S. Khalil-Abad, R. Khajavi, M.E. Yazdanshenas, Fabrication of superhydrophobic polymethylsilsesquioxane nanostructures on cotton textiles by a solution immersion process, J. Colloid Interf. Sci. 359 (2011) 530–535.
[47] C. Bradni, Teoria del restauro, Edizioni di Storia e Letteratura, Rome, (1963).
[48] D. Aslanidou, C. Tsioptsias, C. Panayiotou, A novel approach for textile cleaning based on supercritical CO_2 and pickering emulsions, J. Supercrit. Fluids 76 (2013) 83–93.
[49] S. Kivotidi, C. Tsioptsias, E. Pavlidou, C. Panayiotou, Flame retarded hydrophobic cellulose through impregnation with aqueous solutions and supercritical CO_2, J. Therm. Anal. Calorim. 111 (2013) 475–482.
[50] C. Tsioptsias, C. Panayiotou, Thermal stability and hydrophobicity enhancement of wood through impregnation with aqueous solutions and supercritical carbon dioxide, J. Mater. Sci. 46 (2011) 5406–5411.
[51] P.N. Manoudis, I. Karapanagiotis, A. Tsakalof, I. Zubirtikudis, C. Panayiotou, Superhydrophobic composite films produced on various substrates, Langmuir 24 (2008) 11225–11232.
[52] M.K. Tiwari, I.S. Bayer, G.M. Jursich, T.M. Schutzius, C.M. Megaridis, Highly liquid-repellent, large-area, nanostructured poly(vinylidenefluoride)/poly(ethyl2-cyanoacrylate) composite coatings: particle filler effects, ACS Appl. Mater. Inter. 2 (2010) 1114–1119.
[53] B.J. Basu, V.D. Kumar, Fabrication of superhydrophobic nanocomposite coatings using polytetrafluoroethylene and silica nanoparticles, ISRN Nanotechnology (2011), Article ID 803910.
[54] T.M. Schutzius, I.S. Bayer, G.M. Jursich, A. Das, C.M. Megaridis, Superhydrophobic-superhydrophilic binary micropatterns by localized thermal treatment of polyhedral oligomeric silsesquioxane (POSS)-silica films, Nanoscale 4 (2012) 5378–5385.
[55] B. Leng, Zh. Shao, G. de With, W. Ming, Superoleophobic cotton textiles, Langmuir 25 (2009) 2456–2460.
[56] C. Pirat, M. Sbragaglia, A.M. Peters, B.M. Borkent, R.G.H. Lammertink, M. Wessling, D. Lohse, Multiple time scale dynamics in the breakdown of superhydrophobicity, Europhys. Lett. 81 (2008), Article ID 66002.

[57] M. Sbraggalia, A.M. Peters, Ch. Pirat, B.M. Borkent, R.G.H. Lammertink, M. Wessling, D. Lohse, Spontaneous breakdown of superhydrophobicity, Phys. Rev. Lett. 99 (2007), Article ID 156001.
[58] B. He, N.A. Patankar, H.J. Lee, Multiple equilibrium droplet shapes and design criterion for rough hydrophobic surfaces, Langmuir 19 (2003) 4999–5003.
[59] N.A. Patankar, On the modeling of hydrophobic contact angles on rough surfaces, Langmuir 19 (2003) 1249–1253.
[60] D. Cardon, Natural Dyes-sources Tradition Technology and Science, Archetype Publications Ltd., London, 2007.